

Multi-Year Rayleigh Lidar Temperature Measurement of the Polar Middle Atmosphere at Chatanika

Satyaki Das^(a,b), Richard Collins^(a,b), Jintai Li^(a), V. Lynn Harvey^(c), Brentha Thurairajah^(d)

^(a) Geophysical Institute, University of Alaska, Fairbanks,
Fairbanks, Alaska 99775, USA

^{b)} Department of Atmospheric Sciences, University of Alaska, Fairbanks,
Fairbanks, Alaska 99775, USA

^{c)} Laboratory for Atmospheric and Space Physics, University of Colorado, Boulder
Boulder, CO 80303, USA

^{d)} Center for Space Science and Engineering Research, Virginia Tech,
Blacksburg, VA 24061, USA
sdas8@alaska.edu

Abstract: We present Rayleigh density temperature lidar temperature measurements of the stratosphere and mesosphere that extends over 87 nights from September 2018 to April 2022 made at Chatanika, Alaska (65°N, 147°W). We highlight the wintertime measurements, where sudden stratospheric warming (SSW) events occurred in 2019 and 2021. We focus on the meteorology of the polar stratospheric vortex, the Aleutian anticyclone, the planetary wave activity, and the mean winds. The temperature profiles measured in January and February 2019 reflect the evolution of the SSW and the recovery of the circulation with the disappearance of the stratopause, the appearance near isothermal temperature profile, and the return to a conventional stratopause.

1. Introduction

The wintertime circulation of the Arctic middle atmosphere continues to attract interest due to the occurrence of stratospheric sudden warming events where the circulation is disrupted by breaking planetary waves, resulting in a reversal of the wintertime circulation, with changes in the zonal mean wind, the filtering of gravity waves, and the residual circulation [1]. Temperature observations of the Arctic middle atmosphere (~20 – 80 km) are difficult to acquire due to the small number of ground-based observations and seasonal limitations on space-based measurements. Furthermore, unlike the Antarctic middle atmosphere, the wintertime circulation of the Arctic middle atmosphere is zonally asymmetric [2].

In this study we present recent Rayleigh lidar observations of the Arctic middle atmosphere over central Alaska from September 2018 through April 2022. During this period there are two SSW events in January 2019 and January 2021. We highlight the observations during these periods and document the changes in the nightly temperature profiles.

2. Rayleigh Lidar

A Rayleigh density temperature lidar (RDTL) has operated at Poker Flat Research Range (PFRR), Chatanika, Alaska since 1997. Studies

have focused on the meteorology of the middle atmosphere, with measurements of the stratosphere and mesosphere (~40-80 km) [3,4]. In 2014-2018 the lidar system was progressively upgraded from a single channel receiver with a 0.6 m telescope to a three-channel receiver with a 1.04 m telescope to allow yield higher amplitude signals with greater fidelity than previous studies.

The RDTL raw signal profiles are acquired at a resolution of 50 s and 48 m. The lidar signal is determined from the raw signal from three channels after correction for pulse pile-up and the electronic response of each channel. The lidar signal profile is exponentially smoothed with a 2 km running average to reduce the uncertainty in the signal. The temperature profile assumes a SPARC temperature at 85 km and is integrated downward under the assumption of hydrostatic equilibrium. The temperature profile is then determined from the lidar signal under standard inversion techniques. The lowest altitude of temperature retrieval is chosen at 40 km where there is no contamination from the aerosol. The temperature at an altitude z is calculated by,

$$T(z) = T(z_0) \frac{N(z_0)}{N(z)} \left(\frac{z_0}{z}\right)^2 + \frac{M}{R} \int_z^{z_0} \frac{N(r)}{N(z)} \left(\frac{r}{z}\right)^2 g(r) dr \quad (1)$$

Where z_0 is the reference altitude (85 km), $N(z)$ is the signal profile obtained from RDTL, M is

molecular weight of air, R is the universal gas constant and g is gravitational constant.

The temperature measurements of the Rayleigh lidar extends over 87 nights of observation from September 2018 to April 2022. The data covers months from August to April. As Chatanika is below the Arctic circle, the lidar cannot be operated during May to July due to the lack of nighttime hours in these months. Daily measurements last between 3 to 16 hours for a total of 832 hours. The average observation period lasted 9.5 hours.

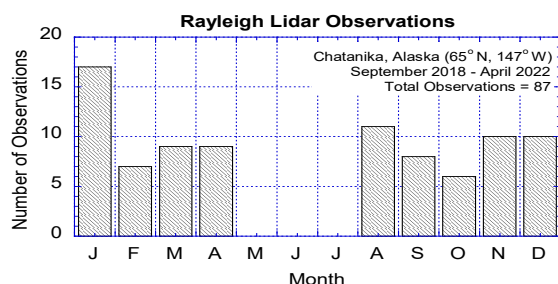


Figure 1. Monthly distribution of lidar measurements.

The monthly distribution of the 87 lidar measurements is plotted in figure 1. The RDTL measurements can only take place under clear sky conditions. The highest number of measurements was made in January (17), and the lowest number of measurements was made in October (6). The low number of observations in October reflects the low number of clear nights in that month.

3. Rayleigh Lidar Temperatures

The nightly mean temperature profiles are plotted in figure 2 by month. Clearly the night-to-night variability is greatest in January and February and lowest in August and September. The August profile is only calculated up to 75 km to avoid any contamination of the lidar signal by the presence of noctilucent, or polar mesospheric, clouds. The profiles are then averaged in each month to form the monthly mean temperature profile. The monthly averaged temperatures from 2018-22 (black) show a stratopause that is least pronounced in January when the temperatures are most variable. The average monthly temperatures in 2018-2022 (black) are in good agreement with the monthly temperatures in 1997-2005 (blue) [2]. The average monthly temperatures from both data sets show similar structure with altitude and generally differ by about the

standard error (green dashed) and within the rms uncertainty (black dashed) of the 2018-2022 data.

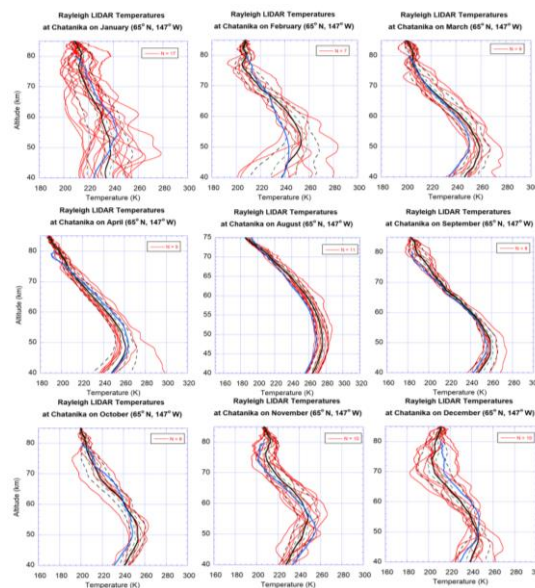


Figure 2. Nightly temperature profiles as a function of altitude at Chatanika, AK.

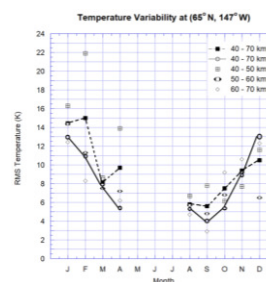


Figure 3. Variation of rms temperature with month at PFRR, Chatanika, Alaska at different altitude ranges.

The monthly variation in rms temperature is plotted in figure 3. The 40-70 km data joined by solid line corresponds to the 1997-2005 temperatures. The rms temperatures are root mean-square averages of the sample standard deviations of the temperature over the altitude range. The yearly mean of the corresponding variability in 2018-22 is 9 K over 40-70 km similar to the variability of 9 K in 1997-2005. The highest variability of 15 K occurs in February and the lowest of 5.5 K in September over the 40-70 km altitude span. However, taking all the altitude spans into consideration, the highest variability of 22 K is observed in February at 40 km-50 km altitude whereas the lowest variability is observed in September with a value of 3 K at 60 km – 70 km altitude.

4. The Arctic Middle Atmosphere

A strong SSW event took place around the first week of January 2019 and a weaker SSW on the first week of January 2021. The SSWs are evident in the winds over Chatanika as determined from the Modern-Era Retrospective analysis for Research and Applications (MERRA-2, figure 4). In the winter 2018-2019 the wind reversal, with westward winds (blue), is evident in the upper mesosphere in the end of December and progresses downward in the first three weeks of January. The zero-wind line extends down to 20 km. The SSW is followed by strong eastward winds (red-yellow). In the winter of 2020-2021 there again is a reversal of the winds that is more variable than in 2019-2020 but extends down to below 20 km. The reversal in 2020-21 is preceded by a period of strong eastward winds. The reversal of the winds in winter 2021-2022 is characteristic of a late season warming when the winter circulation weakens at the beginning of summer.

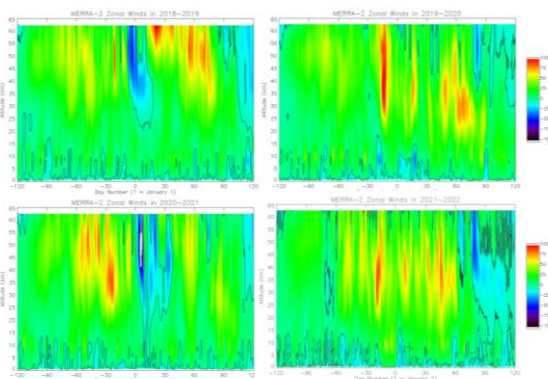


Figure 4. Zonal winds over from MERRA-2 over Chatanika in 2018-19 (upper left) 2019-20 (lower left), 2020-21 (upper right), 2021-22 (lower right).

The synoptic structure of the polar stratospheric vortex and Aleutian anticyclone are identified [5]. The changes in the structure of the polar stratospheric vortex (color coded) and Aleutian anticyclone (black) reflect the changes in the winds. In figure 5 the vortex is clearly split in January 2019 during the wind reversal, while it remains robust in 2020, splits again in 2020 during the wind reversal, and remains robust in 2021. The red line indicates the lidar at Chatanika. The planetary wave activity (not shown) is consistent with the structure of the synoptic systems when the wave activity is

stronger the vortex and anticyclone are more intertwined.

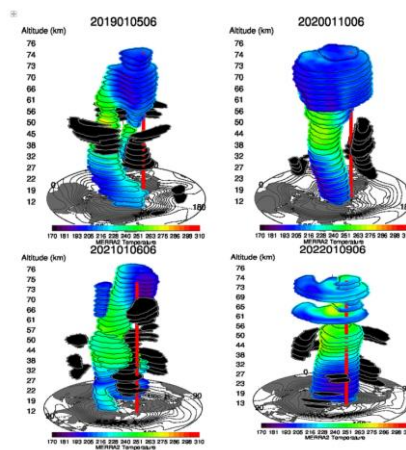


Figure 5. The structure of the Arctic polar stratospheric vortex and Aleutian anticyclone at 0600 UT on 5, 10, 6, and 9 January 2019, 2020, 2021, and 2022 respectively.

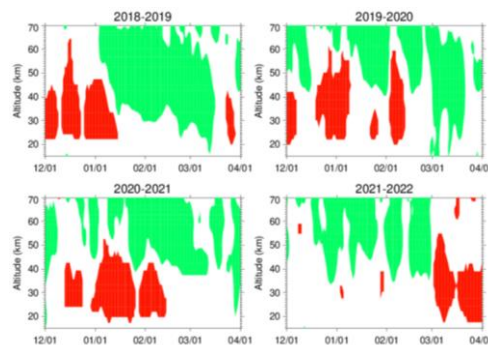


Figure 6. Evolution of polar vortex (green) and Aleutian anticyclone (red) over Chatanika in 2018-19 (upper left) 2019-20 (lower left), 2020-21 (upper right), 2021-22 (lower right).

In figure 6, we identify the presence of the polar vortex and Aleutian anticyclone over Chatanika. In 2018-19 the anticyclone is dominant over Chatanika in December and during the SSW in January, but the vortex becomes dominant after the SSW. The vortex recovers with strong winds over Chatanika in mid-January. This situation is contrasted with 2022-22 when the vortex is present throughout December, January, and February and the anticyclone is absent. In 2019-20 and 2020-21 the winds reflect the synoptic conditions with stronger eastward winds when the vortex is overhead, and weaker eastward and westward winds associated with the presence of the anticyclone.

The lidar temperature profiles reflect the synoptic meteorology over Chatanika. In 2018-

2019 the evolution of the temperature profiles shown in figure 7 follows the disturbance due to the SSW with the formation of an elevated stratosphere and subsequent recovery of the middle atmosphere. A stratopause is clearly present in the late-December. During the SSW event on 4 January 2019 and 6 January 2019 the stratopause disappears, the temperature decreases in the 40-67 km range and local temperature maximum is present appears near 80 km. On 17 January (190117) as the eastward winds recover and the vortex reappears, the temperature increases in the 40-60 km region and decreases above that but there is still no obvious stratopause. On 21 January (190121) as the recovery continues, the stratopause reappears at around 80 km altitude. On 1 February (190201) the stratopause descends to 58-65 km altitude range and the stratosphere has returned to its typical state following the SSW event. The middle atmosphere over Chatanika goes from being dominated by the presence of the Aleutian anticyclone before the SSW to being dominated by the stratospheric vortex after the SSW. In 2020-2021 a weak stratopause is observed early during the wind reversal and a near isothermal temperature profile is observed during the latter stage of the wind reversal.

In 2019-20 and 2021-22 the temperature profiles are variable but the persistent near isothermal behavior observed in 2018-2019 is not observed.

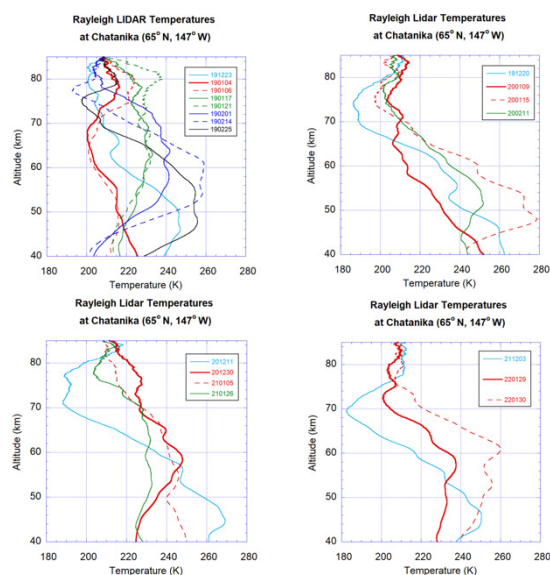


Figure 7. Rayleigh lidar temperature profiles on nights from the winters of 2018-19 (Top left), 2019-20 (Top right), 2020-21 (Bottom left) and 2021-22 (Bottom right).

5. Conclusions

We report new measurements of the Arctic middle atmosphere over Alaska in 2018-2022. The measurements show similar behavior seasonal behavior as earlier multi-year measurements in 1997-2005. The night-to-night variability is much greater in winter than in late summer and early fall. The temperature behavior in the winter over Chatanika reflects the large-scale meteorology. During the SSW in 2018-2019 the temperature structure follows a clear progression where the stratopause disappears and reforms. In the other winters the evolution of the stratopause is more variable. However, the stratopause remains more pronounced in the winters of 2019-20 and 2021-22 when there is no SSW.

The impact of the meteorology reported here will be used to investigate the modulation of gravity wave activity during SSWs in a companion paper.

6. References

- [1] M. R. Schoeberl, D. L. Hartmann, “The dynamics of the stratospheric polar vortex and its relation to springtime ozone depletion,” in *Science*, 251, 46–52 (1991).
- [2] A. Chandran, R. L. Collins, V. L. Harvey, “Stratosphere-mesosphere coupling during stratospheric sudden warming events,” in *Advances in Space Research*, 53, 1265-1589, (2014).
- [3] B. Thuraijah, R.L. Collins, K. Mizutani, “Multi-year temperature measurements of the middle atmosphere at Chatanika, Alaska (65°N, 147°W),” in *Earth, Planets and Space*, 61, 755–764 (2009).
- [4] B. K. Irving, R. L. Collins, R. S. Lieberman, B. Thuraijah, K. Mizutani. “Mesospheric inversion layers at Chatanika, Alaska (65 °N, 147 °W): Rayleigh lidar observations and analysis,” in *Journal of Geophysical Research Atmospheres*, 11235–1124119, (2014).
- [5] V.L. Harvey, R. B. Pierce, T. D. Fairlie, M. H. Hitchman, “A climatology of stratospheric polar vortices and anticyclones,” in *Journal of Geophysical Research Atmospheres*, 107, 4442 (2002).